

## Transition to $\Delta$ matter from hot, dense nuclear matter within a relativistic mean field formulation of the nonlinear $\sigma$ and $\omega$ model

Zhuxia Li,<sup>1,2</sup> Guangjun Mao,<sup>2,3</sup> Yizhong Zhuo,<sup>1,2</sup> and Walter Greiner<sup>3</sup>

<sup>1</sup>China Institute of Atomic Energy, P.O. Box 275(18), Beijing 102413, People's Republic of China

<sup>2</sup>Institute of Theoretical Physics, Academia Sinica, P.O. Box 2735, Beijing 100080, People's Republic of China

<sup>3</sup>Institut für Theoretische Physik, Frankfurt University, D-60054 Frankfurt am Main, Germany

(Received 9 January 1997)

An investigation of the transition to  $\Delta$  matter is performed based on a relativistic mean field formulation of the nonlinear  $\sigma$  and  $\omega$  model. We demonstrate that in addition to the  $\Delta$ -meson coupling, the occurrence of the baryon resonance isomer also depends on the nucleon-meson coupling. Our results show that for the favored phenomenological value of  $m^*$  and  $K$ , the  $\Delta$  isomer exists at baryon density  $\sim 2-3\rho_0$  if  $\beta=1.31$  is adopted. For universal coupling of the nucleon and  $\Delta$ , the  $\Delta$  density at baryon density  $\sim 2-3\rho_0$  and temperature  $\sim 0.4-0.5 \text{ fm}^{-1}$  is about normal nuclear matter density, which is in accord with a recent experimental finding. [S0556-2813(97)07408-6]

PACS number(s): 25.75.Dw, 13.75.Cs, 24.10.Cn, 21.65.+f

### I. INTRODUCTION

One of the central aims of high-energy heavy ion collisions is to understand the properties of hadronic matter at high temperature and densities. Hadronic matter may have a rich structure under high compression and at high excitation energies. There are conjectures about abnormal nuclear matter (such as resonance isomers) at high density,  $\rho \approx 3-5\rho_0$ . Relativistic mean field calculations, using an extended Walecka Lagrangian with nonlinear  $\sigma$  field, predict that the nuclear equation of state may yield a second minimum at about  $\rho \approx 3\rho_0$  if the  $\Delta$  resonance is introduced [1]. Furthermore, it has been pointed out that the existence of the density isomer can change several observables substantially, especially particle production yields [2].

In Ref. [1] it was shown that the appearance of a second minimum as well as its exact position and depth depend on the scalar and vector coupling constant of the  $\Delta$ . However, the investigation is limited to only one parameter set which leads to the saturation properties of nuclear matter with compressibility  $K=344 \text{ MeV}$ , effective mass  $m_N^*/m_N=0.678$  at the saturation density  $\rho=0.17 \text{ fm}^{-3}$  for which the compressibility is too large. It is now known that an accurate mean-field equation requires  $0.6 \leq m^*/m \leq 0.65$  and  $200 \leq K \leq 280 \text{ MeV}$  in order to reproduce reasonable energy systematics, spin-orbit splittings, and deformation in finite nuclei [3-5]. It has been pointed out that the parameter set is rather restrictive for compressibility within a favorable region  $K=200-300 \text{ MeV}$  for the Walecka type model with nonlinear  $\sigma$  field. Bodmer has introduced a self-interaction vector field in addition to the nonlinear scalar field [3] into the effective Lagrangian, which has been found to be important for accurately modeling the self-energies and consequent nuclear properties. This approach introduces a density dependence that goes beyond what is included in nonrelativistic Brueckner theory. With this model the properties for both finite nuclear systems and the saturation properties of nuclear matter can be well described simultaneously [6,7]. Furthermore, inclusion of the vector meson quartic self-interaction

makes it possible to fit  $K$  and  $m^*$  with positive  $c$ , particularly for the favored phenomenological values of  $m^*/m_N \approx 0.6$ ,  $K \approx 200-300 \text{ MeV}$  [3-5] and to give a large softening of the nuclear equation of state (EOS). Therefore, the model also provides a means to study the influence of different parameter sets corresponding to different saturation properties of nuclear matter on the nuclear EOS when a  $\Delta$  resonance is introduced. In addition, recent experiments have indicated that large numbers of  $\Delta$ 's are produced in the reaction zone of heavy ion collisions at beam energies of 1-2 GeV/nucleon [8,9]. Therefore, it becomes more interesting to reinvestigate the problem of the transition to  $\Delta$  matter based on a model which can accurately model nuclear properties. The aim of this paper is to study the properties of hot, dense nuclear matter, mainly the behavior of the energy per baryon, the effective mass, the density of nucleons and  $\Delta$ 's versus the baryon density at various temperatures when a  $\Delta$  resonance is introduced via a relativistic mean field formulation of the nonlinear  $\sigma$ - $\omega$  model introduced by Bodmer. We pay special attention to the problem of the transition to  $\Delta$  matter. The outline of the paper is as follows: in the next section we will briefly introduce the theoretical framework and in Sec. III we present our results and summary.

### II. THEORETICAL FRAMEWORK

The effective Lagrangian can be written as

$$\mathcal{L} = \mathcal{L}_F + \mathcal{L}_I. \quad (1)$$

Here  $\mathcal{L}_F$  is the Lagrangian density for free nucleon,  $\Delta$ , and meson fields

$$\begin{aligned} \mathcal{L}_F = & \bar{\psi}(i\gamma_\mu \partial^\mu - m_N)\psi + \bar{\psi}_{\Delta\nu}(i\gamma_\mu \partial^\mu - m_\Delta)\psi_\Delta^\nu \\ & + \frac{1}{2}\partial_\mu\sigma\partial^\mu\sigma - U(\sigma) - \frac{1}{4}\omega_{\mu\nu}\omega^{\mu\nu} + U(\omega), \end{aligned} \quad (2)$$

and  $U(\sigma)$ ,  $U(\omega)$  are the self-interaction part of the scalar field and vector field

$$U(\sigma) = \frac{1}{2}m_\sigma^2\sigma^2 + \frac{1}{3}b(g_\sigma\sigma)^3 + \frac{1}{4}c(g_\sigma\sigma)^4, \quad (3)$$

TABLE I. The parameter sets used in the calculation as well as the corresponding saturation properties of nuclear matter.  $m_\sigma=550$  MeV and  $m_\omega=783$  MeV are used for all cases.

	$g_\sigma$	$g_\omega$	$b$	$c$	$Z$	$E_{\text{bin}}$	$m_N^*/m_N$	$K$ (MeV)	$\rho_0$
set 1	9.187	10.425	6.641	2.047	$\infty$	-15.84	0.678	344	0.17
set 2	11.77	13.88	13.447	10.395	3.655	-15.75	0.6	200	0.1484
set 3	11.32	13.87	1.279	50.645	3.655	-15.75	0.6	300	0.1484
set 4	10.285	11.73	8.3553	83.33	2.0602	-15.75	0.7	200	0.1484
set 5	8.52	9.049	-6.5472	312.6	1.5476	-15.75	0.8	200	0.1484

$$U(\omega) = \frac{1}{2} m_\omega^2 \omega_\mu \omega^\mu \left( 1 + \frac{g_\omega^2}{2} \frac{\omega_\mu \omega^\mu}{Z^2} \right), \quad (4)$$

$$m_\Delta^* = m_\Delta - g_\sigma^\Delta \sigma. \quad (7)$$

respectively.  $\mathcal{L}_I$  is the interaction Lagrangian density

$$\begin{aligned} \mathcal{L}_I &= \mathcal{L}_{NN} + \mathcal{L}_{\Delta\Delta} + \mathcal{L}_{\Delta N} = g_\sigma \bar{\psi}(x) \psi(x) \sigma(x) \\ &\quad - g_\omega \bar{\psi}(x) \gamma_\mu \psi(x) \omega^\mu(x) + g_\sigma^\Delta \bar{\psi}_{\Delta\nu}(x) \psi_\Delta^\nu(x) \sigma(x) \\ &\quad - g_\omega^\Delta \bar{\psi}_{\Delta\nu}(x) \gamma_\mu \psi_\Delta^\nu(x) \omega^\mu(x), \end{aligned} \quad (5)$$

where  $\psi_{\Delta\mu}$  is the Rarita-Schwinger spinor of the  $\Delta$  baryon. The symbols and notation have their usual meaning [10]. It should be noticed that in addition to the cubic and quartic self-interaction of the scalar field, a quartic self-interaction of the vector field has also been introduced according to the suggestion of Bodmer [3]. The coupling strengths of  $g_\sigma$ ,  $g_\omega$ , and  $b$ ,  $c$ ,  $Z$  used in the calculations are given in Table I. The set 1 is taken as the same one used in [1] and the others are from [3]. Little is known about the  $\Delta$  coupling strengths  $g_\sigma^\Delta$  and  $g_\omega^\Delta$ . Usually, parameters  $\alpha$  and  $\beta$  defined as  $\alpha = g_\sigma^\Delta/g_\sigma$ ,  $\beta = g_\omega^\Delta/g_\omega$  are introduced instead of  $g_\sigma^\Delta$  and  $g_\omega^\Delta$ . There are several choices for  $\alpha$  and  $\beta$ : (1) universal coupling constant for nucleon and  $\Delta$ , i.e.,  $\alpha = \beta = 1$ , based on the quark counting argument [11,12], (2)  $\alpha = \beta = 1.31$ , assuming that the coupling strengths show a splitting similar to the mass splitting of  $\Delta$  and nucleon, (3)  $\alpha = 1$  and  $\beta = 1.31$  since the  $\omega$  meson has a real quark-antiquark structure while the  $\sigma$  meson has not, and (4) the recent calculations with the QCD sum rule method yield  $\alpha \approx 0.5$ , while no prediction for  $\beta$  [13]. The choices of (1), (3), and (4) will be investigated in this paper. The choice (2) will not be investigated considering the arguments of (3) and (4).

For symmetric, infinite isotropic nuclear matter the following equations of motion for the model can be derived within mean field approach:

$$\begin{aligned} (i \gamma_\mu \partial^\mu - m_N^* - g_\omega \gamma_\mu \omega^\mu) \psi &= 0, \\ (i \gamma_\mu \partial^\mu - m_\Delta^* - g_\omega^\Delta \gamma_\mu \omega^\mu) \psi^\Delta &= 0, \\ m_\sigma^2 \sigma + b(g_\sigma \sigma)^2 + c(g_\sigma \sigma)^3 &= g_\sigma \rho_s, \\ m_\omega^2 \omega_0 \left( 1 + g_\omega^2 \frac{\omega_0^2}{Z^2} \right) &= g_\omega \rho_b, \end{aligned} \quad (6)$$

where,

$$m_N^* = m_N - g_\sigma \sigma,$$

The scalar density  $\rho_s$  and vector density  $\rho_b$  are the sum of the nucleon and  $\Delta$  scalar and vector densities, respectively:

$$\rho_s = \rho_s(N) + \beta \rho_s(\Delta),$$

$$\rho_b = \rho_B(N) + \alpha \rho_B(\Delta). \quad (8)$$

The thermodynamic potential for a system at finite temperature is written as

$$\begin{aligned} \Omega &= -T \ln Z = [U(\sigma) - U(\omega)]V \\ &\quad - T \left[ \sum_{k,\lambda} \ln(1 + e^{-(E_N^* + g_\omega \omega_0 - \mu)/T}) \right. \\ &\quad + \sum_{k,\lambda} \ln(1 + e^{-(E_N^* + g_\omega \omega_0 + \mu)/T}) \\ &\quad + \sum_{k,\lambda} \ln(1 + e^{-(E_\Delta^* + \alpha g_\omega \omega_0 - \mu)/T}) \\ &\quad \left. + \sum_{k,\lambda} \ln(1 + e^{-(E_\Delta^* + \alpha g_\omega \omega_0 + \mu)/T}) \right], \end{aligned} \quad (9)$$

where

$$E_i^* = \sqrt{k^2 + m_i^{*2}}. \quad (10)$$

The thermodynamic functions can be derived from the thermodynamic potential. The baryon density is written as

$$\begin{aligned} \rho_B &= -\frac{1}{V} \frac{\partial \Omega}{\partial \mu} = \sum_i \frac{\gamma(i)}{(2\pi)^3} \int d^3k [n_i(T) - \bar{n}_i(T)] \\ &= \rho_B(N) + \rho_B(\Delta), \end{aligned} \quad (11)$$

where  $\gamma(i) = 4, 16$  for  $i = N, \Delta$ , respectively, with

$$\begin{aligned}
n_N(T) &= \frac{1}{(1 + e^{(E_N^* + g_\omega \omega_0 - \mu)/T})}, \\
\bar{n}_N(T) &= \frac{1}{(1 + e^{(E_N^* + g_\omega \omega_0 + \mu)/T})}, \\
n_\Delta(T) &= \frac{1}{(1 + e^{(E_\Delta^* + \alpha g_\omega \omega_0 - \mu)/T})}, \\
\bar{n}_\Delta(T) &= \frac{1}{(1 + e^{(E_\Delta^* + \alpha g_\omega \omega_0 + \mu)/T})}.
\end{aligned} \tag{12}$$

Here it should be noticed that  $\rho_B$  is not equal to  $\rho_b$  when  $\alpha \neq 1$ . The conserved quantity is  $\rho_B$  but not  $\rho_b$ .  $\rho_b$  serves as the source term of the vector field. From Eqs. (11) and (12)  $\rho_s(i)$  and  $\rho_B(i)$  can be expressed as

$$\begin{aligned}
\rho_s(i) &= \frac{\gamma(i)}{(2\pi)^3} \int d^3k \frac{m^*}{(k^2 + m^{*2})^{1/2}} [n_i(T) + \bar{n}_i(T)], \\
\rho_B(i) &= \frac{\gamma(i)}{(2\pi)^3} \int d^3k [n_i(T) - \bar{n}_i(T)], \\
i &= N, \Delta.
\end{aligned} \tag{13}$$

The energy is given by

$$\epsilon = \epsilon_B + \epsilon_\sigma + \epsilon_\omega, \tag{14}$$

with

$$\begin{aligned}
\epsilon_B &= \sum_i \frac{\gamma(i)}{(2\pi)^3} \int d^3k (k^2 + m_i^{*2})^{1/2} [n_i(T) + \bar{n}_i(T)], \\
i &= N, \Delta, \\
\epsilon_\sigma &= U(\sigma), \\
\epsilon_\omega &= g_\omega \rho_b \omega_0 - \frac{1}{2} m_\omega^2 \omega_0^2 \left( 1 + \frac{g_\omega^2 \omega_0^2}{2 Z^2} \right).
\end{aligned} \tag{15}$$

The pressure can be derived as

$$P = - \left. \frac{\partial \Omega(T, V, \mu)}{\partial V} \right|_{T, \mu} = P_B + P_\sigma + P_\omega, \tag{16}$$

with

$$\begin{aligned}
P_B &= \sum_i \frac{\gamma(i)}{(2\pi)^3} \int d^3k \frac{k^2}{(k^2 + m_i^{*2})^{1/2}} [n_i(T) + \bar{n}_i(T)], \\
P_\sigma &= -U(\sigma), \\
P_\omega &= U(\omega).
\end{aligned} \tag{17}$$

The nucleon and delta effective mass  $m_N^*$  and  $m_\Delta^*$ , respectively, have to satisfy the self-consistency relation:

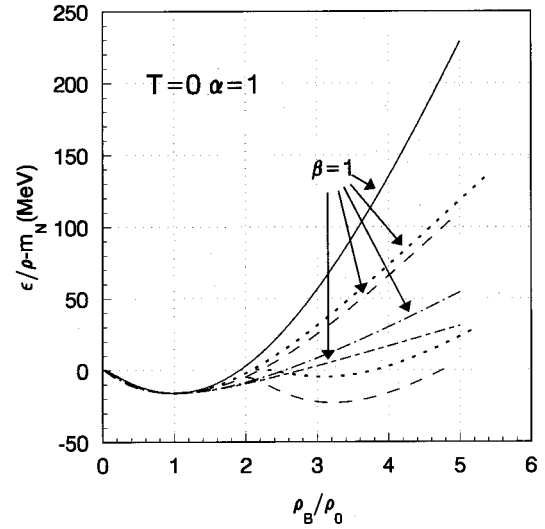


FIG. 1. The energy per baryon as a function of the baryon density at zero temperature. The solid, dashed, pointed, dash-pointed, long-short dashed lines correspond to the results calculated with set 1–set 5 given in Table I, respectively. The results for  $\beta=1$  are pointed by arrow and others are for  $\beta=1.31$ . The results with set 5 for both  $\beta=1$  and  $\beta=1.31$  are the same

$$\begin{aligned}
m_N^* - m_N + C_s \left( \rho_s - \frac{b}{g_\sigma^3} (m_N^* - m_N)^2 + \frac{c}{g_\sigma^4} (m_N^* - m_N)^3 \right) &= 0, \\
m_\Delta^* - m_\Delta - \beta (m_N^* - m_N) &= 0.
\end{aligned} \tag{18}$$

To compute the thermodynamic functions, one first specifies  $T$  and  $\mu$ . The self-consistency relation (18) and field equations (6) are then solved to determine the effective masses  $m_N^*$  and  $m_\Delta^*$  as well as  $\omega_0$ . Then the energy and pressure can be evaluated through Eqs. (11), (14), and (16).

### III. NUMERICAL RESULTS AND SUMMARY

In Fig. 1 we show the energy per baryon as a function of density (“EOS”) at  $T=0$  for various cases with  $\alpha=1$ ,  $\beta=1$  and 1.31 and parameter sets 1–5 given in Table I. Comparing the results for  $\beta=1$  and  $\beta=1.31$ , we find that the “EOS” strongly depends on the  $\Delta$ -meson coupling. I.e., there is no second minimum for the cases with  $\beta=1$ , while for  $\beta=1.31$  a second minimum (i.e., the  $\Delta$  isomer) may occur. In addition, we find that the appearance of a second minimum as well as its position and depth also strongly depends on the nucleon-meson coupling, which is fixed by the saturation properties of nuclear matter characterized by the effective mass  $m^*$  and compressibility  $K$ . This can be seen from Fig. 1 by comparing the results with different parameter sets. Another important feature is that the introduction of the quartic term of vector field obviously favors the appearance of a second minimum due to its effect of softening the EOS at high density. For instance, the EOS calculated with set 1, for which the vector meson field has no quartic term, has no second minimum for  $\beta=1.31$  (also see [1]), while for other cases with the quartic term of the vector field introduced (set 2–5 given in Table I) all have second minima

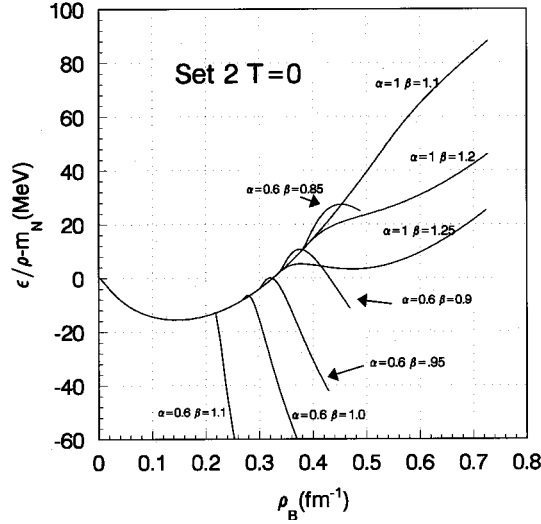


FIG. 2. The same as Fig. 1, but for various  $\alpha$  and  $\beta$  with parameter set 2 only.

except the case with set 5 which has large effective mass  $m_N^*/m_N=0.8$ .

Now let us further analyze how the appearance of a second minimum as well as its position and the depth are correlated with the saturation properties of nuclear matter when  $\beta = 1.31$  is adopted. In order to investigate the dependence on the effective mass, let us compare the ‘‘EOS’’ calculated with parameter sets 2, 4, 5, which have the same  $K=200$  MeV, but different effective masses  $m_N^*/m_N=0.6, 0.7,$  and  $0.8$ , respectively. For the first two cases, there exist a second minimum, but for set 4 the minimum is much shallower and at much higher density than that for set 2. For set 5, with large  $m_N^*/m_N=0.8$ , there is no second minimum. In fact, in the case of set 5 the ‘‘EOS’’ follows the same curve for both  $\beta=1$  and  $\beta=1.31$  and the  $\Delta$  density remains zero as the baryon density increases. The results clearly imply that the small saturated effective mass favors the appearance of a second minimum. For the cases of set 2 and 3, which correspond to the same effective mass ( $m_N^*/m_N=0.6$ ), but different compressibility  $K=200, 300$  MeV, respectively, a second minimum is obtained at almost the same position ( $\rho_B/\rho_0 \approx 3$ ) for both cases, but the depth of the second minimum is different. For set 2 with  $K=200$  MeV, the second minimum is lower than that of set 3 with  $K=300$  MeV and even lower than the first minimum. That means that with a given effective mass the depth of the second minimum depends on the saturated compressibility  $K$ . With smaller values of  $K$ , the second minimum becomes deeper. Moreover, the difference between the ‘‘EOS’’ calculated with  $\beta=1.31$  is larger than that calculated with  $\beta=1$ . That means that the influence of the compressibility on the ‘‘EOS’’ is stronger when  $\beta=1.31$  than that when  $\beta=1$ .

In order to further investigate the influence of the  $\Delta$  coupling constants on the ‘‘EOS,’’ we compare the results with different choices of  $\alpha$  and  $\beta$ , but the same parameter set (we take set 2). In Fig. 2 we show the energy per baryon as a function of  $\rho_B$  at zero temperature for different  $\Delta$  coupling constants. The calculations are carried out for  $\alpha=0.6$  suggested by the QCD sum rule calculations [13]. In this case

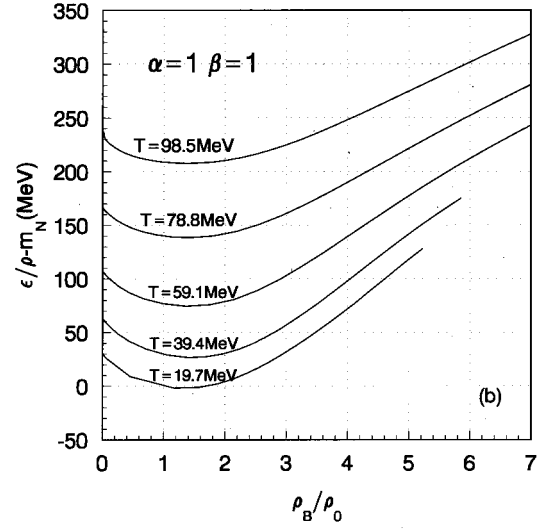
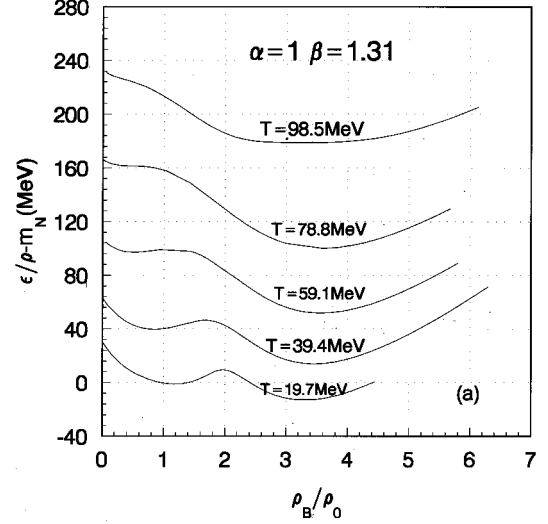


FIG. 3. (a) The energy per baryon as a function of the baryon density at temperature  $0.1-0.5 \text{ fm}^{-1}$  with set 2 and  $\beta=1.31$ . (b) The energy per baryon as a function of the baryon density at temperature  $0.1-0.5 \text{ fm}^{-1}$  with set 2 and  $\beta=1.0$ .

$\rho_b$  is smaller than baryon density  $\rho_B$  since  $\alpha$  is much smaller than unity, consequently, a weaker repulsion is produced by  $\omega$  meson according to Eq. (6). The calculated results for  $\alpha=0.6$  show that when  $\beta-\alpha \geq 0.35$  (i.e., for cases of  $\alpha=0.6, \beta=0.95, 1.0, 1.1$ ) the interaction is too attractive and the energy per baryon starts to decrease at  $\rho_B=1.5-2.5 \rho_0$  and then becomes very negative. It implies that the difference between  $\alpha$  and  $\beta$  should not be too large. For smaller  $\beta$  ( $=0.9$  and  $0.85$ ) the second minimum happens at higher density. For  $\alpha=1$ , there is no second minimum if  $\beta$  is smaller than  $1.25$ . We will only take  $\alpha=1$ , the usual value, in the following calculations and thus,  $\rho_B$  is always equal to  $\rho_b$ .

Figures 3(a) and 3(b) show the energy per baryon as a function of the baryon density at temperatures  $0.1-0.5 \text{ fm}^{-1}$  (i.e.,  $T=19.7, 39.4, 59.1, 78.8, 98.5$  MeV) with parameter set 2 and  $\beta=1.31$  and  $\beta=1$ , respectively. For  $\beta=1.31$ , for lower temperature ( $T \leq 0.3 \text{ fm}^{-1}$ ), the behavior is similar to that with zero temperature given in Fig. 1, ex-

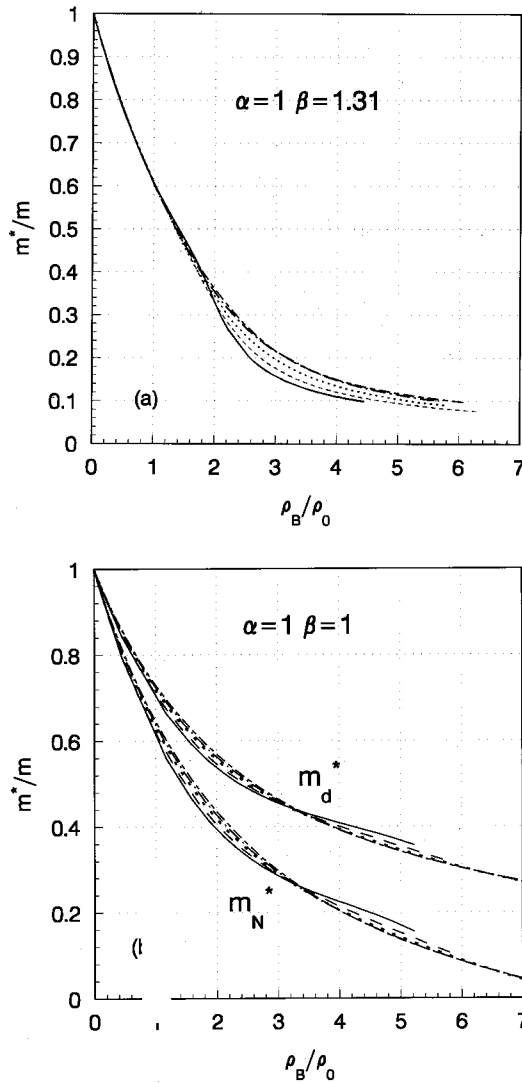


FIG. 4. The effective mass as a function of the baryon density for nucleon and  $\Delta$  at temperature  $T=0.1$ – $0.5$  fm $^{-1}$ , respectively calculated with set 2 and  $\beta=1.31$ . The solid, dashed, pointed, dash-pointed, long-short dashed lines correspond to the temperatures  $T=0.1, 0.2, 0.3, 0.4, 0.5$  fm $^{-1}$ . (b) The effective mass as a function of the baryon density for nucleon and  $\Delta$ , at temperature  $0.1$ – $0.5$  fm $^{-1}$  with set 2 and  $\beta=1.0$ . The solid, dashed, pointed, dash-pointed, long-short dashed lines correspond to the temperatures  $T=0.1, 0.2, 0.3, 0.4, 0.5$  fm $^{-1}$ , respectively.

cept that the first minimum shifts a little to lower density. It means that at this regime the density dependence is more important than the temperature dependence. As the temperature increases, when  $T \geq 0.4$  fm $^{-1}$ , the first minimum disappears and the second minimum remains. For the  $\beta=1$  case shown in Fig. 3(b), there is no change in the behavior, i.e., there is only one minimum at the normal nuclear matter density, which means that there is no  $\Delta$  resonance isomer for this case.

In Figs. 4(a) and 4(b), we show the behavior of the effective mass of the nucleon and the  $\Delta$  versus the baryon density for temperatures  $0.1$ – $0.5$  fm $^{-1}$ . Figure 4(a) corresponds to  $\beta=1.31$  and Fig. 4(b) corresponds to  $\beta=1$ . For  $\beta=1.31$ , the effective mass of the nucleon and the  $\Delta$  follows the same curves for various temperatures. For  $\beta=1$ , the effective

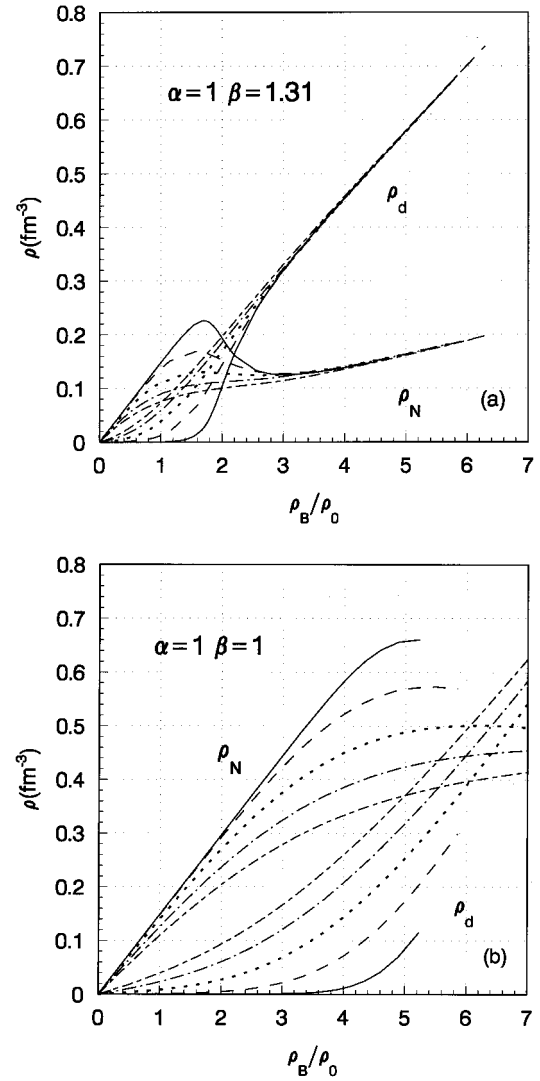


FIG. 5. (a) The nucleon and  $\Delta$  density as a function of the baryon density at temperature  $0.1$ – $0.5$  fm $^{-1}$  with set 2 and  $\beta=1.31$ . The solid, dashed, pointed, dash-pointed, long-short dashed lines correspond to the temperatures  $T=0.1, 0.2, 0.3, 0.4, 0.5$  fm $^{-1}$ , respectively. (b) The nucleon and  $\Delta$  density as a function of the baryon density at temperature  $T=0.1$ – $0.5$  fm $^{-1}$  with set 2 and  $\beta=1.0$ . The solid, dashed, pointed, dash-pointed, long-short dashed lines correspond to the temperatures  $T=0.1, 0.2, 0.3, 0.4, 0.5$  fm $^{-1}$ , respectively.

mass of the  $\Delta$  is always larger than that of the nucleon for various temperatures and they follow different curves. The different behavior of the effective mass for  $\beta=1.31$  and  $\beta=1.0$  is closely related to the different behavior of the energy per baryon versus the baryon density and temperature.

Since the transition to  $\Delta$  matter is characterized by the rapid increase of the  $\Delta$  density, in Figs. 5(a) and 5(b) we show the dependence of the  $\Delta$  density  $\rho_{\Delta+\bar{\Delta}}$  and the nucleon density  $\rho_{N+\bar{N}}$  on the baryon density at different temperatures for  $\beta=1.31$  and  $\beta=1$ , respectively. Since the number of antiparticles is negligible in most cases studied here, we have  $\rho_{\Delta+\bar{\Delta}} \sim \rho_\Delta$  and  $\rho_{N+\bar{N}} \sim \rho_N$ . For  $\beta=1.31$  [Fig. 5(a)], it can be seen that at temperatures  $T=0.1$ – $0.3$  fm $^{-1}$  the nucleon density first increases then reaches the maximum around  $\rho_B/\rho_0=1.5$  and then decreases accompanied by a rapid

increase in the  $\Delta$  density. At  $\rho_B/\rho_0$  around 1.5–2.5 the  $\Delta$  density exceeds the nucleon density. At temperature  $T \geq 0.4 \text{ fm}^{-1}$ , the rising slope of the nucleon density becomes smaller and the maximum disappears, and then the  $\Delta$  density quickly exceeds the nucleon density around  $\rho_B = \rho_0$ , which coincides with the disappearance of the first minimum of “EOS” in Fig. 3(a). For the  $\beta=1$  case shown in Fig. 5(b), the behavior of the nucleon and  $\Delta$  density versus the baryon density is very different from that of  $\beta=1.31$ . In this case, the nucleon density first increases very fast as the baryon density increases and saturates at  $\rho_B \approx 5\rho_0$  for low temperatures. As the temperature increases, the rising slope of the nucleon density decreases and the  $\Delta$  density starts to increase at much lower density. For all temperatures, the nucleon density remains larger than that of  $\Delta$  until very high baryon density, which is closely related to the behavior of the “EOS” for this case shown in Fig. 3(b). Here we have noticed that at  $T=0.4\text{--}0.5 \text{ fm}^{-1}$  the  $\Delta$  density reaches about  $1/3\text{--}1/2$  of nucleon density at baryon density around  $2\text{--}3 \rho_0$ . I.e., at this condition the  $\Delta$  density already reaches the normal nuclear matter density, which seems to be in agreement with the recent experimental finding mentioned in the Introduction [8,9]. In this case the average spacing between  $\Delta$ 's is comparable with the nucleon spacing in normal nuclear matter. Our result may suggest the occurrence of  $\Delta$  matter at the temperature  $T=0.4\text{--}0.5 \text{ fm}^{-1}$  and baryon density around  $2\text{--}3 \rho_0$ , which has nothing to do with the  $\Delta$  isomer.

In summary, we have presented the behavior of the effective mass, the energy per baryon as well as the nucleon and  $\Delta$  densities versus the baryon density at different temperatures for various parameter sets corresponding to different saturation properties of nuclear matter. The dependence of

the “EOS” on the nucleon-meson and  $\Delta$ -meson coupling constants as well as the self-interaction of  $\sigma$  and  $\omega$  meson at zero temperature are studied carefully. The results show that the appearance of the density isomer not only depends on the  $\Delta$ -meson coupling, i.e.,  $\alpha$  and  $\beta$ , but also depends on the nucleon-meson coupling. More specifically, the appearance of the density isomer and its corresponding baryon density is strongly correlated with the effective mass at saturation, while the depth of the second minimum is influenced by the compressibility  $K$ . From our calculations, we can conclude that for the favored phenomenological values of the effective mass and compressibility required by the properties of nuclear matter as well as finite nuclei, i.e.,  $0.6 \leq m^*/m \leq 0.65$  and  $200 \leq K \leq 280 \text{ MeV}$  [3–5], the density isomer exists at baryon density  $\approx 2\text{--}3\rho_0$ , if  $\beta=1.31$  is adopted. For universal coupling of the  $\Delta$  and nucleon, no density isomer appears. But for the later case (universal coupling case) the  $\Delta$  density at baryon density  $\rho=2\text{--}3 \rho_0$  and temperature  $T=0.4\text{--}0.5 \text{ fm}^{-1}$  almost reaches the normal density of nuclear matter, which is in agreement with that of the recent experimental finding [8,9]. Further experimental tests, such as those predicted by Ref. [2], are necessary in order to determine whether there exists a second minimum in the nuclear equation of state. This might also provide direct information about the  $\Delta$ -meson coupling constants, according to our investigation.

#### ACKNOWLEDGMENTS

This work was supported by National Natural Science Foundation of China (No. 19375070 and No. 19675069) and Science Foundation of Nuclear Industry of China.

- 
- [1] B. M. Waldhauser, J. Theis, J. A. Maruhn, H. Stöcker, and W. Greiner, *Phys. Rev. C* **36**, 1019 (1987).
  - [2] C. Hartnack, J. Aichelin, H. Stöcker, and W. Greiner, *Phys. Rev. Lett.* **72**, 3767 (1994).
  - [3] A. R. Bodmer, *Nucl. Phys.* **A526**, 703 (1991).
  - [4] S. Gmuca, *Nucl. Phys.* **A547**, 447 (1992); *Z. Phys. A* **342**, 387 (1992).
  - [5] Y. Sugahara and H. Toki, *Nucl. Phys.* **A579**, 557 (1994).
  - [6] R. J. Furnstahl *et al.*, *Phys. Rev. C* **36**, 2500 (1987).
  - [7] R. J. Furnstahl and B. D. Serot, *Phys. Rev. C* **37**, 2338 (1993).
  - [8] M. Appenheimer *et al.*, GSI Annual reports, 1995.
  - [9] M. Averbeck *et al.*, GSI Annual reports, 1994.
  - [10] B. D. Serot and J. D. Walecka, *Adv. Nucl. Phys.* **16**, 1 (1986).
  - [11] S. A. Mosozkowski, *Phys. Rev. D* **9**, 1613 (1974).
  - [12] S. I. A. Garpman *et al.*, *Nucl. Phys.* **A322**, 382 (1979).
  - [13] X. Jin, *Phys. Rev. C* **51**, 2260 (1995).